AD-A184 995 ON THE ACCURACY OF TURBULENT BASE FLOW PREDICTIONS(U) 1/1
NIELSEN ENGINEERING AND RESEARCH INC MOUNTAIN VIEW CA
R E CHILDS ET AL. 10 JUN 87 ARO-22354.1-EG-S
UNCLASSIFIED DAAL03-86-C-0002 F/G 20/4 NL

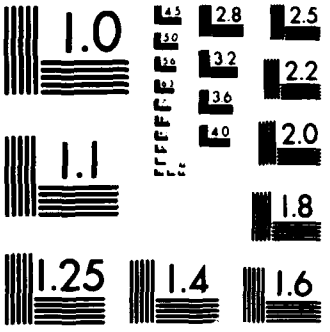

UNCLASSIFIED MASTER COPY - FOR REPRODUCTION PURPOSES

SECURITY CLASSIFICATION OF THIS PAGE

RT DOCUMENTATION PAGE

1a. R **AD-A184 995**

1b. RESTRICTIVE MARKINGS DTIC FILE COPY

2a. S

3. DISTRIBUTION / AVAILABILITY OF REPORT
Approved for public release; distribution unlimited.

2b. DECLASSIFICATION / DOWNGRADING SCHEDULE

4. PERFORMING ORGANIZATION REPORT NUMBER(S)

5. MONITORING ORGANIZATION REPORT NUMBER(S)
ARO 22354.1-EG-S

6a. NAME OF PERFORMING ORGANIZATION
Nielsen Engineering & Research, Inc

6b. OFFICE SYMBOL (If applicable)

7a. NAME OF MONITORING ORGANIZATION
U. S. Army Research Office

6c. ADDRESS (City, State, and ZIP Code)
Nielsen Engineering &Research, Inc.
Mountaion View, CA 94043-2287

7b. ADDRESS (City, State, and ZIP Code)
P. O. Box 12211
Research Triangle Park, NC 27709-2211

8a. NAME OF FUNDING / SPONSORING ORGANIZATION
U. S. Army Research Office

8b. OFFICE SYMBOL (If applicable)

9. PROCUREMENT INSTRUMENT IDENTIFICATION NUMBER
DAAL03-86-C-0002

8c. ADDRESS (City, State, and ZIP Code)
P. O. Box 12211
Research Triangle Park, NC 27709-2211

10. SOURCE OF FUNDING NUMBERS

PROGRAM ELEMENT NO.	PROJECT NO.	TASK NO.	WORK UNIT ACCESSION NO.

11. TITLE (Include Security Classification)
On the Accuracy of Turbulent Base Flow Predictions

12. PERSONAL AUTHOR(S)
R. E. Childs, S. C. Caruso

13a. TYPE OF REPORT	13b. TIME COVERED FROM ____ TO ____	14. DATE OF REPORT (Year, Month, Day)	15. PAGE COUNT
Reprint			

16 SUPPLEMENTARY NOTATION
The view, opinions and/or findings contained in this report are those of the author(s) and should not be construed as an official Department of the Army position, policy, or decision, unless so designated by other documentation.

17 COSATI CODES		
FIELD	GROUP	SUB-GROUP

18. SUBJECT TERMS (Continue on reverse if necessary and identify by block number)

19 ABSTRACT (Continue on reverse if necessary and identify by block number)

Abstract on reprint

20 DISTRIBUTION / AVAILABILITY OF ABSTRACT
☐ UNCLASSIFIED/UNLIMITED ☐ SAME AS RPT. ☐ DTIC USERS

21. ABSTRACT SECURITY CLASSIFICATION
Unclassified

22a NAME OF RESPONSIBLE INDIVIDUAL

22b. TELEPHONE (Include Area Code)

22c. OFFICE SYMBOL

DD FORM 1473, 84 MAR 83 APR edition may be used until exhausted. All other editions are obsolete.

SECURITY CLASSIFICATION OF THIS PAGE
UNCLASSIFIED

AIAA'87

AIAA-87-1439
On the Accuracy of Turbulent Base Flow Predictions

R.E. Childs and S.C. Caruso, Nielsen Engineering and Research, Mountain View, CA

AIAA 19th Fluid Dynamics, Plasma Dynamics and Lasers Conference

June 8-10, 1987/Honolulu, Hawaii

On the Accuracy of Turbulent Base Flow Predictions

Robert E. Childs* and Steven C. Caruso*
Nielsen Engineering and Research, Inc.
510 Clyde Ave, Mountain View CA 94043.

Abstract

Flow in the afterbody region of a supersonic vehicle with propulsive jets is difficult to predict accurately partly because the complex pattern of shocks, expansion fans, and free shear layers is difficult to resolve, and partly because the turbulence is difficult to model. The problems of numerical resolution and turbulence modeling are addressed, and it is shown that, while insufficient resolution causes some errors, larger errors can be attributed to the turbulence model. The standard k-ϵ model gives good results for one set of experimental data, despite its inability to model many effects on the turbulence which may be present in the base region. A modification for Mach number effects is derived and verified against experimental data for plane shear layers. When the modified model is used in the computation of the base flow, the predicted base pressure rises significantly. This suggests that good results with the standard k-ϵ model, or any model which does not predict Mach number effects, are due to fortuitous error cancellation.

Introduction

A simple bluff base flow consists of a reversed flow region adjacent to the base which is bounded by a propulsive jet and the freestream, as sketched in Fig. 1. The base pressure and the shape of the reversed flow region are determined by several competing mechanisms. Entrainment into the freestream and propulsive jet pumps fluid out of the reversed flow region. The outer shear layer, which emanates from the "shoulder," is moderately thick and turbulent. The inner shear layer, which originates at the nozzle lip, is initially very thin and probably laminar, at least in non-combusting laboratory experiments. Often there is greater mixing in the outer shear layer which induces a preferred rotation in the base region (clockwise in the sense of Fig. 1). The flow in the base region is at relatively low speed, and thus this region is roughly at uniform pressure. Expansion fans emanating from the shoulder of the base and the lip of the nozzle cause the base pressure to be substantially below the freestream, for the configuration shown. This produces base drag, which can be an appreciable part of a vehicle's total drag. The low pressure adjacent to the base pulls fluid from the region where the shear layers merge and the pressure is slightly higher, to make up for fluid lost to entrainment. Base flows result from a rather complex balance between these competing mechanisms, all of which must be computed accurately if good predictions are to be obtained.

The ability of contemporary Navier-Stokes methods to predict this type of flow was investigated by Petrie and Walker,[1] who compared true predictive calculations by several workers[2,3,4] to experimental data. Not only did the predictions give poor agreement with the experiment, but also there were significant variations in the results from nominally similar prediction methods. All methods which used the Baldwin-Lomax[5] model underpredicted the base pressure, and the one method which used the k-ϵ or k-W models overpredicted the base pressure. The importance of good grid clustering was demonstrated. More recent computations[6,7,8] of the low-pressure-ratio experiment of Petrie and Walker have focused on grid resolution, while still using the Baldwin-Lomax model, and have given improved results for the base pressure. However, significant grid dependence was seen in the solutions, and thus, the predictive capability of the mathematical model cannot be evaluated. At this time the ability to predict accurately the type of base flow sketched in Fig. 1 has not been demonstrated.

Putnam and Bissinger[9] reviewed predictions for a wide range of nozzle afterbody flows. They observed that Navier-Stokes methods gave poor results downstream of separation. Thus, bluff base flows and the associated drag were not predicted very well. One of their conclusions was that Navier-Stokes methods are not reliable for the prediction of afterbody drag.

The difficulties in obtaining accurate numerical predictions fall into two general categories. The first is the problem of computing accurate solutions to the partial differential equations (PDEs) used to model the physics, which, in the present work, are the compressible Reynolds-averaged Navier-Stokes equations with a k-ϵ turbulence model. The second area concerns the accuracy with which the mathematical representation models the physics. Particular interest focuses on the turbulence model. Within these two general areas, there are several aspects relevant to base flows.

The problem of obtaining accurate solutions to the model equations centers on several narrow regions (at shocks, expansion corners, and in free shear layers) where the solution varies rapidly in an otherwise smooth flow. Strong normal and oblique shocks must be computed without excessive numerical smearing or oscillations. Pre-shock Mach numbers in excess of five are seen in the present work, and even higher Mach numbers will be present in other applications. The thin shear layers bordering the recirculating flow region need to be resolved so that the mean flow and the turbulence quantities (when a multi-equation model is used) are unaffected by numerical diffusion. The expansions at the sharp corners of the base often cause numerical difficulties and may give rise to unusual and unexpected separation characteristics. Turbulence in the base region is difficult to measure, and it is poorly understood. It is affected by pressure gradients, including interactions with shocks and expansions, streamline curvature, the merging of shear layers, and high Mach numbers. Individually, these effects are somewhat understood yet still difficult to model; together they may produce entirely unexpected behavior. Present models cannot be relied on to give reasonably accurate predictions over a wide ranges of conditions.

* Research Scientist, Member AIAA.

Progress has been made in some of these areas. Differencing schemes with good shock capturing abilities have been developed (e.g. Ref. 10,11). Adaptive grid methods have demonstrated the ability to give good clustering in regions of high gradients (e.g. Ref. 2). The area which will likely be the most difficult to solve to the point at which reliable accurate engineering calculations can be made is that of turbulence modeling.

It should be noted that accurate measurements in the base region are also difficult to obtain. Because of the high Mach numbers, there are density and temperature fluctuations which reduce the accuracy of hot wire anemometry. Laser based instruments may also be affected by fluctuations in the optical density, as well as particle seeding and particle lag problems, especially in the high speed, low density regions of the plume. Shadowgraph-type visualizations, surface oil flows, and surface pressures probably yield the most reliable data from these flows at present, despite their limitations.

The objectives of the present work are to evaluate the dependence of solutions on the numerical grid used, to determine what must be done to eliminate any significant grid dependence, and to assess and improve upon the accuracy of turbulence modeling for the base region.

In the remainder of this report the following will be described: the numerical method, the turbulence model, including a modification for Mach number effects, and the grid generation method. Then the results of several calculations will be discussed.

Navier-Stokes Algorithm

A finite volume algorithm, with a characteristic-based method of computing fluxes and an implicit time advance method, is used to solve the compressible Reynolds-averaged Navier-Stokes equations and the k-ϵ turbulence model equations. A brief description of the distinguishing aspects of the method is given below. The algorithm and code used in the present work were developed by Coakley, and the reader is referred to Ref. 12 for details of the method.

Base flows often contain complex patterns of shocks, and it is desirable to resolve these sharply, without excessive numerical diffusion. There is a broad class of algorithms for inviscid flow,[10,11] often referred to as high resolution methods, which have very good shock capturing abilities. Strong shocks can be captured over two or three grid points with little or no oscillation in the solution, which removes the need to do case specific grid clustering to obtain well defined captured shocks. Coakley's method for inviscid flux calculations falls into this class, and it uses upwind characteristic differencing, with first, second, or third order spatial accuracy. Optionally, second order central differencing can be used. Except where noted, the second order upwind method is used for inviscid fluxes. Viscous terms are always computed with second order central differencing.

The second order upwind difference scheme is described here. For this discussion, the equations are linearized so that a brief yet clear explanation of the differencing scheme can be given. The one-dimensional Euler equations can be expressed as

$$Q_t + F_x = 0, \quad Q = [\rho, \rho u, \rho e], \quad F = [\rho u, \rho u^2 + p, (\rho e + p)u] \qquad (1)$$

in which ρ is density, u is velocity, e is specific internal energy, $p = (\gamma-1)(e-u^2/2)$ is pressure, and γ is the ratio of specific heats.

The concern is with the approximation of F_x. The flux vector F can be split into components, F^+ and F^-, associated with signals moving in the $+x$ and $-x$ directions, with the property $F = F^+ + F^-$. The split is accomplished by expressing F as AQ, in which $A = \partial F/\partial Q$, and by performing eigenvector manipulations on A. (The linear assumption means that A is spatially invariant.) F_x is, in effect, computed by conventional second order upwind differences applied to F^+ and F^-.

$$F_x = \frac{1}{2\Delta x}[F^+_{i-2} - 4F^+_{i-1} + 3F^+_i - 3F^-_i + 4F^-_{i+1} - F^-_{i+2}] \qquad (2)$$

In actual application in the finite volume method for the nonlinear case, the differencing scheme has a very different appearance, and the details of the application are crucial to the methods properties. Steady solutions of the Navier-Stokes equations are obtained by time asymptotic integration with a factored implicit method. A spatially variable time step is used. Again, the reader is referred to Ref. 12 for details on the method.

Turbulence Model

One possible approach to modeling the turbulence in the base region is to adopt the most "advanced" model which is practical to use and hope that it captures the critical turbulence mechanisms. The Reynolds-stress transport model (RSTM) is an example of an advanced model which will capture some complex turbulence mechanisms, and for certain types of flows, a RSTM will likely give very good results. However, it can be inferred from Ref. 13 that the "standard" RSTM does not predict high Mach number effects nor does it predict accurately the curving and merging shear layers, for example. Ad hoc modifications would be required to predict these and other phenomena which are expected. Ad hoc modifications can also be used to improve a less complex model, which may then be more practical and less expensive to use than the advanced model. Either approach introduces additional adjustable coefficients, and neither approach has shown clearly superior results for the types of flows which are of interest here. Thus, the approach taken here is to use the k-ϵ model as the basis upon which to develop an improved model.

Two turbulence models are used in the present work: the "standard" high Reynolds number k-ϵ model[14] and the same model with a modification to account for the effects of Mach number. The former is not presented here; only the modification for high Mach numbers is covered. There are effects other than those due to Mach number which should also be included in a model for base flows. These will be studied in the future.

The starting point for the high Mach number modification is the RSTM of Bonnet (Ref. 13, pp. 1408-1410). Bonnet derived an expression for the compressible, return-to-isotropy part of the pressure-strain term, which is similar to its incompressible analogue. By assuming pressure fluctuations are small relative to density fluctuations, the model for the complete pressure-strain term (compressible and incompressible parts) is reduced to the incompressible form with a scale factor which depends on the mean Mach number. On the strength of plausible arguments, the scale factor is made to depend on the Mach number of the fluctuating velocity, $\overline{u'u'}/a^2$, where a is the acoustic speed.

However, the algebraic form of the scale factor is unchanged. The scale factor has one coefficient, which was optimized by numerical experiment, and then the model gave good results for the spreading rate of a planar free shear layer up to M = 7. For M > 7 Bonnet's numerical method was not stable.

In the present work, Bonnet's model is reduced to a form compatible with an eddy-viscosity model, such as the k-ϵ model. To do this, it is assumed that the flow is subject to homogeneous shear and that $\overline{u'u'}/k = 0.96$, which is an average of this parameter for uniform shear flow and isotropic turbulence in incompressible flow. With these assumptions and the RSTM coefficients $C_1 = 1.8$ and $C_2 = 0.6$ (see e.g. Ref. 13) in Bonnet's model, the compressibility modification used in the present work is determined. It is a modification of C_μ.

$$C_\mu = C_{\mu 0} (1 + C_{c1} k/a^2)(1 + C_{c2} k/a^2)^{-2} \qquad (3)$$

in which $C_{c1} = 8.4$ and $C_{c2} = 6.5$. As with with the standard k-ϵ model, $C_{\mu 0} = 0.09$, and the eddy-viscosity is $\nu_t = C_\mu \rho k^2/\epsilon$. The variation of $C_\mu/C_{\mu 0}$ with $\sqrt{k}/a$ is given in Fig. 2. The accuracy of Eq. (3) is evaluated through calculations of the spreading rate of a plane free shear layer, which are discussed in the Results section. It should be emphasized that the only numerical optimization done in the development of Eq. (3) was that done by Bonnet. It is suspected that Eq. (3) may underpredict shear stresses at very high Mach numbers, but this was not studied in the present work. Future work may include optimizing C_{c1} and C_{c2}.

Also shown in Fig. 2 is the compressibility correction used by Pergament et al.,[15] which was derived on a purely empirical basis. Their compressibility correction differs from the present one in two major ways. It predicts a more rapid onset of Mach number effects. This is at least partially due to the assumption in the present work about the ratio of $\overline{u'u'}/k$. If $\overline{u'u'}/k$ had been assumed to be that for uniform shear flow, then $C_\mu/C_{\mu 0}$ would decrease more rapidly with increasing Mach number. Secondly, their method bases the correction on k_{max}, the maximum value of turbulence kinetic energy at an axial station, whereas the present method uses the local value of turbulence energy.

Boundary Conditions

Boundary conditions must be supplied at inflow stations and along solid walls. Far field and downstream conditions are remote from the base and do not affect the solution in the base region. Inflow conditions for the external flow are supplied from experimental data at a measurement station upstream of the base. The freestream and much of the external boundary layer flow are supersonic, as is the jet exit flow. Therefore, all inflow variables are prescribed. The external boundary layer is approximated as a 1/7th power law mean velocity profile, and the density and turbulence quantities are consistent with an adiabatic, zero pressure gradient boundary layer.

At all solid walls the viscous no-slip condition is applied to mean flow velocities, the pressure is extrapolated linearly, and there is a zero temperature gradient. The shear stress at the wall and k and ϵ at the first point away from the wall are determined by incompressible "wall function" boundary conditions, which are based on the assumptions that the velocity profile is logarithmic and that the production of turbulence kinetic energy equals its dissipation. For the flows considered here, wall function boundary conditions are as accurate as can be obtained with any approach. Furthermore, in the base region, turbulence mechanisms in the free shear layers are dominant, and the turbulence model boundary conditions should have a weak effect on the solution.

Grid Generation

It has become clear that some form of solution adaptive grid clustering is desirable in order to obtain accurate solutions affordably. Deiwert et al.[2] have developed a rather general method for clustering grid points in regions of high gradients, and they have applied the method to base flows. Venkatapathy and Lombard[7] have used this procedure in an approach that employs adaptive and overlapping grids for base flows. Despite these efforts, grid independent solutions are very elusive.

Accurate solutions to the governing equations are obtained by providing grid clustering which is sufficient to eliminate significant truncation errors at flow features which must be resolved. In the present work it is observed that shocks require minimal clustering because their internal structures are irrelevant for the present purposes and because the differencing scheme has good shock capturing abilities. However, free shear layers (and perhaps expansions) require significant grid clustering because their internal structures must be resolved. Denser grid clustering may be required at free shear layers for the k-ϵ model than for zero-equation turbulence models (e.g., Baldwin-Lomax), since k and ϵ vary more rapidly through the layer than do mean flow quantities. Therefore, the objective of the present approach is to provide the greatest clustering for the free shear layers bounding the recirculating flow, which also gives good clustering at the expansion corners. No special clustering is done at shocks. By focussing only on the shear layers, it is possible to generate grids without excessive skewing or rapid variations in clustering, which can degrade accuracy.

A grid generation procedure has been developed that makes use of the fact that the crucial shear layers in the base flows considered here have a relatively simple geometry. The shear layers emanating from the jet exit and the shoulder of the body are initially very thin and relatively straight. They form two sides of the triangular shaped base region. (This approach is similar to concepts in component models for base flows.) The grid generation method specifies "control surfaces," which follow the shear layers as they depart from the base, as sketched in Fig. 3(a). At the control surfaces the radial grid clustering is specified, and exponential stretching is used to expand the clustering away from the control surfaces.

Where the layers merge, the control surfaces are forced to maintain separation by requirements imposed on the radial grid spacing. Downstream of the merging zone the grid relaxes to roughly uniform spacing in the radial direction, within the plume. Clustering is used in the axial direction near the base. The axial grid spacing is kept moderately small until somewhat downstream of the Mach disk, at which location the flow is entirely supersonic. The minimum grid spacing on the base and the body is selected to achieve $y^+_{min} \simeq 50$, for application of wall function boundary conditions.

Figure 3(b) gives the grid in the base region for the specific flow displayed in Figs. 4-6. Looking ahead to Fig. 5, it can be seen that the grid clustering follows the shear layers of the solution. Most grids used in the present work are very similar to that shown in Fig. 3(b). For grid refinement studies, which are given later, the total number of grid points, and thus the absolute grid density, is changed, but the character of the grid is generally similar.

At present the grid generation procedure is not automated, nor is it applied concurrently with the Navier-Stokes method. However, there are no fundamental research issues blocking these advances. The present procedure is used by first obtaining a converged flow solution, and then using that solution to guide the generation of a new grid. The approach is inefficient for computational costs, but it minimizes development costs. Since no research efforts, including the present one or Refs. 2 or 7, have demonstrated grid independent solutions, there seems little impetus to develop a production-type procedure at this time.

Results

Results are presented to demonstrate the accuracy of the method and to show specific areas where more work is needed. The two major topics involve the effects of the grid and of the turbulence modeling on the accuracy of the solutions.

The afterbody experiments reported by Petrie and Walker[1] are used for comparison. These flows involve an cylindrical afterbody with a centered axisymmetric jet in a M = 1.4 freestream. The external boundary layer at a station 3.2 body radii upstream of the base is 0.14 body radii thick, with $Re_\delta = 9.0 \times 10^4$. The propulsive jet emerges from a conical 10° half-angle nozzle which has a design exit Mach number of M = 2.7; the ratio of nozzle exit radius to body radius is 0.2. Inflow boundary conditions at the nozzle exit plane are consistent with experimental stagnation conditions and ideal inviscid conical flow in the nozzle. Data were reported at two nozzle pressure ratios, NPR = 2.15 and NPR = 6.44. Initially, some results are given for both cases to demonstrate the capabilities of the method. Then a more detailed investigation of the factors which influence the accuracy of the solution are presented, for the NPR = 2.15 case. Results for the variation of the spreading rate of the plane free shear layer with respect to Mach number are also given.

Figure 4 gives the base pressures computed by the present method and other Navier-Stokes methods and measured in the experiment, for the NPR = 2.15 case. The present result is reasonably accurate, and it predicts a relatively uniform base pressure which is a significant feature of the experimental results.

Except for the present results, the results in Fig. 4(a) were reported in Ref. 1. The results in Fig. 4(b)[6,7,8] have been presented since the publication of Ref. 1. It must be noted that the other calculations shown in Fig. 4(a) were performed "blind." That is, those performing the calculations[3,4,5] were given operating conditions and inflow boundary data, but other experimental data were withheld. The blind test results give a strong indication that the predictive capability for this flow is poor. The present results were obtained with prior knowledge of experimental results, but that knowledge was not used to improve the accuracy of the calculation. The present solution was obtained on the third calculation of this flow (after two grid refinements). Of the many solutions computed for this flow, this one is believed to be the best approximation to the solution of the PDEs which model the flow because it is on the finest grid. The present solution is weakly grid dependent, which will be discussed later. The initial calculation on a coarser grid gives a better prediction of the base pressure (shown in Fig. 13), but it is believed to be a less accurate solution of the model PDEs.

A comparison between the predicted Mach number contours and the experimental shadowgraph in Fig. 5 indicates that the general features of the flow are captured accurately. A clear distinction between the barrel shock and the jet shear layer is visible in the Mach number contours but not in the experimental shadowgraph or velocity field (shown below). The location of the Mach disk is well predicted. The computed maximum Mach number in the jet is between 5.0 and 5.5, which is greater than the measured maximum of about M = 3.5. It is not known if this discrepancy is significant since uncertainty estimates for the Mach number measurements are not given. The Mach number may be sensitive to changes in velocity in this range, depending on how the acoustic speed is determined.

Velocity vectors, given in Fig. 6, reveal discrepancies between experiment and computation in the recirculating flow, which are believed to be significant. In the computation, the reverse flow velocity is too large, the outer shear layer spreads too rapidly, and the vortical nature of the recirculation is different. These discrepancies are small for the present case, but they indicate the potential for larger errors in predictions of other cases. The recirculating base flow is driven by the turbulent stresses, and thus, these errors suggest shortcomings in the turbulence model or inadequate resolution in the shear layers.

Results for the case with NPR = 6.44 are discussed briefly before further comments on the NPR = 2.15 case are given. The base pressures from experiment and previous blind predictions[1] and from the present effort are given in Fig. 7. The experimental shadowgraph and the predicted Mach number contours are compared in Fig. 8. The present results give a reasonable prediction of the average base pressure and the overall structure of the flow field.

However, the strong expansion at the lip of the nozzle causes large oscillations in the pressure. A repeat calculation on a different grid gave a significantly different solution. The problem lies in the method's inability to capture the expansion at the nozzle exit which is too fine to be resolved on the grid employed. The computational nozzle exit flow does not have a physically correct boundary layer, but rather it has a two point transition zone between the uniform conical jet flow and the nozzle lip. The validity of this approximation is not known. The physical nozzle boundary layer is very thin, so that resolving it can be a severe computational burden. Time constraints did not permit a study of the problems at the strong expansion; therefore, the NPR = 6.44 case was not investigated further. Future work will address this problem. The expansion problem is also present in the NPR = 2.15 case, but it is confined to a few grid points near the nozzle lip and the global solution is independent of changes to the grid near the lip. For the NPR = 2.15 case the expansion problem can be ignored while other aspects of the calculation are investigated.

Effects of Grid Resolution

A major concern is to determine the accuracy with which the numerical solution approximates the exact solution of the model PDEs. For purposes of research, it would be desirable to produce solutions to the model PDEs which are independent of the grid and numerical discretization scheme, except perhaps in the neighborhoods of discontinuities. A grid dependence study was performed in an effort to determine if the present results were primarily due to fortuitous grid choice or if they are representative of the grid-independent solution of the model PDEs. Fig. 9 gives the base pressures obtained for the three different grids used in the grid refinement study and an additional grid which was specifically generated to give poor clustering in critical regions. The changes in base pressure are less than +/- 5% relative to freestream static pressure, but grid independence is not achieved. Furthermore, the base pressure does not display a monotonic trend as the grid is refined. Thus, it is not possible to estimate the base pressure for an asymptotically fine grid, but also, there is no indication that the base pressure will change significantly as the grid is further refined.

A disconcerting aspect of the present results is that they disagree with a previous result[1] (contributed by the Lockheed group[4]) obtained with a k-ϵ turbulence model. Initial speculation was that inadequate grid clustering and first order upwind differencing on k and ϵ used in Ref. 4 were the cause. A central difference calculation was run on a grid similar to that used by the Lockheed group with a large amount of artificial dissipation added to the k and ϵ equations to mimic the first order differencing. Strong diffusive effects on k and ϵ were observed, but the resulting base pressure was not significantly closer to the Lockheed results. The blind cases were run at $M_\infty = 1.343$, (due to a measurement error which was later corrected), but a calculation at $M_\infty = 1.343$ also failed to produce better agreement with the Lockheed results. Hence, there is a significant difference between the present results and a previous calculation, obtained with a similar method, which cannot readily be explained.

Additional calculations were run for the NPR = 2.15 case, in which central differencing with varying amounts of artificial dissipation was used. Central differencing degrades shock capturing but should not affect the accuracy with which smooth fields, such as the shear layers, are computed. The base pressures for these and all other solutions mentioned are given in Fig. 10. This gives an estimate of the uncertainty in the base pressure, roughly +/- 5%, which can be attributed to effects of the grid and the differencing scheme. Comparison of Figs. 4 and 10 suggests that effects of the grid and the inviscid differencing scheme cannot account for differences in base pressure between present and other[1,6,7,8] results.

Effects of the Turbulence Model

In the remainder of the results section, the effect of Mach number on the turbulence model is considered. The modification to the k-ϵ model to account for Mach number effects, Eq. (3), was incorporated in the method, and calculations of a planar free shear layer at several Mach numbers and of the NPR = 2.15 base flow were performed.

The spreading rate of the planar free shear layer was selected as a test case at the Stanford Conference on Complex Turbulent Flows.[13] There were two sets of results submitted to the conference. The results from the algebraic-stress two-equation k-ω model used by Wilcox gave poor results and showed no change of spreading rate with Mach number. Bonnet's RSTM showed good agreement with data up to $M_\infty \simeq 7$.

The spreading rate, as defined in Ref. 13, given by the modified k-ϵ model was evaluated by performing calculations of a spatially evolving shear layer for a range of Mach numbers. The inflow conditions were of a flat plate turbulent boundary layer at $Re_\delta = 9 \times 10^4$. The fluid on the low speed side of the shear layer was at rest, and it had the same pressure and stagnation temperature as the freestream. The spreading rate was evaluated at a downstream distance of $x/\theta_0 = 300$ (θ_0 is the initial momentum thickness), at which point the spreading rate was nearly constant with respect to distance. The spreading rate given by the modified k-ϵ model is shown in Fig. 11. The spreading rate at $M = 0$ is $d\delta/dx = 0.10$, which is slightly below the experimental value 0.115. (This was actually run at $M = 0.5$ with the Mach number modification removed.) This underprediction is consistent with k-ϵ results presented at the Stanford conference and reflects the fact that the k-ϵ model coefficients are optimized for a variety of flows, not just the plane free shear layer. The computed spreading rate follows the trend of the experimental data and is in good agreement at $M = 5$. The model underestimates Mach number effects slightly, but in general, it gives a good approximation to the spreading rate of the free shear layer for $M \lesssim 5$.

The modified model was applied to the prediction of the NPR = 2.15 case, and the base pressure is given in Fig. 12. With the modified model, the shear stress and the entrainment in the shear layers decrease. This causes the predicted base pressure to rise by 8% relative to freestream, so that it is in rather poor agreement with experimental base pressure. Other data (not shown) indicate that the reverse flow region is now too long, and that a subsonic region between the jet plume and the freestream extends far downstream, which is also contrary to experimental data. There are several points which should be learned from this result.

Comparison of Figs. 10 and 12 reveals that the change of base pressure caused by one modification to the turbulence model (+8%) is comparable to the change in pressure which was induced by changes to the grid and the difference scheme (+/- 5%). The need for other modifications to the model is justifiable. Thus, the uncertainty in the present base flow calculations due to turbulence modeling is at least equivalent to that due to numerical resolution. It is difficult to argue that the Mach number modification is inappropriate for this flow or that it is grossly in error for the plane shear layer. Thus, there must be additional errors in the standard k-ϵ model that cancel the errors due to Mach number effects. It is unlikely that this cancellation will occur in a wide range of flows. Thus, good results obtained with the standard k-ϵ model, or any model which fails to predict Mach number effects, should be viewed as fortuitous.

As shown in Figs. 4 and 7, most prediction methods which use the Baldwin-Lomax model underpredict the base pressure. If a Mach number modification similar to Eq. (3) were applied to the Baldwin-Lomax model, then the predicted base pressures would likely rise and, on average, give better agreement with experimental data.

Summary

A Navier-Stokes prediction method which is distinguished by an upwind characteristic differencing scheme for inviscid fluxes and a k-ϵ turbulence model was used to investigate the accuracy of base flow calculations. Grid-independent solutions were not obtained. However, grid dependence was shown to be small relative to that seen in previous work and comparable to the uncertainty in the solution due to the turbulence model. Despite its many shortcomings for supersonic base flows, the standard high-Reynolds number k-ϵ model gave good predictions of base pressure and many other aspects of the flowfield.

However, when the model was modified to account for high Mach number effects, the accuracy of the base flow calculation was degraded. This suggests that hidden error cancellation is present in calculations with the standard k-ϵ model. If this is true, then similar conclusions apply to other methods. Good results for high speed flows from any method which does not include Mach number effects on turbulence may be fortuitous.

Acknowledgements

The authors gratefully acknowledge support from the Army Research Office, through contract DAAL03-86-C-0002, and from the NASA Ames Research Center for access to computer facilities. Appreciation is extended to Dr. T. Coakley for the use of his computer code.

References

1. Petrie, H. L. and Walker, B. J., "Comparison of Experiment and Computation for a Missile Base Region Flowfield with a Centered Propulsive Jet," AIAA-85-1618.

2. Deiwert, G. S, Andrews, A. E., and Nakahashi, K., "Theoretical Analysis of Aircraft Afterbody Flow," AIAA-84-1524.

3. Sahu, J. and C. J. Nietubitz, "Numerical Computation of Base Flow for a Missile in the Presence of a Centered Jet," AIAA-84-0527.

4. Thomas, P. D., Reklis, R. P., Roloff, R. R., and Conti, R. J., "Numerical Simulation of Axisymmetric Base Flow on Tactical Missiles with Propulsive Jet," AIAA-84-1658.

5. Baldwin, B. S. and Lomax, H., "Thin Layer Approximation and Algebraic Model for Separated Turbulent Flows," AIAA-73-0257.

6. Lombard, C. K., Luh, R. C.-C., Nagaraj, N., Bardina, J., and Venkatapathy, E., "Numerical Simulation of Backward Step and Jet Exhaust Flows," AIAA-86-0432.

7. Venkatapathy, E. and Lombard, C. K., "Accurate Numerical Simulation of Jet Exhaust Flows with CSCM for Adaptive Overlapping Grids," AIAA-87-0465.

8. Hoffman, J. J., Birch, S. F., and Hopcraft, R. G., "Navier-Stokes Calculations of Rocket Base Flows," AIAA-87-0466.

9. Putnam, L. E. and Bissinger, N. C., "Results of AGARD Assessment of Prediction Capabilities for Nozzle Afterbody Flows," AIAA-85-1464.

10. Roe, P. L., "Characteristic-Based Schemes for the Euler Equations," Ann. Rev. Fluid Mech., Vol. 18, 1986, pp. 337-365.

11. Harten, A., "High Resolution Schemes for Hyperbolic Conservation Laws," J. Comp. Phys., Vol. 49, 1983, pp. 357-393.

12. Coakley, T. J., "Implicit Upwind Methods for the Compressible Navier-Stokes Equations," AIAA J., Vol. 23, No. 3, 1985, pp. 374-380.

13. Kline, S. J. et al., eds., "The 1980-81 AFOSR-HTTM-Stanford Conference on Complex Turbulent Flows," Stanford University, 1981.

14. Launder, B. E. and Spaulding, D. B., "The Numerical Computation of Turbulent Flows," Computer Meth. in App. Mech. and Engrg. 3, 1974, pp. 169-189.

15. Pergament, H. S., Dash, S. M., and Varma, A. K., "Evaluation of Turbulence Models for Rocket and Aircraft Plume Flowfield Predictions," AIAA-79-0356.

Figures

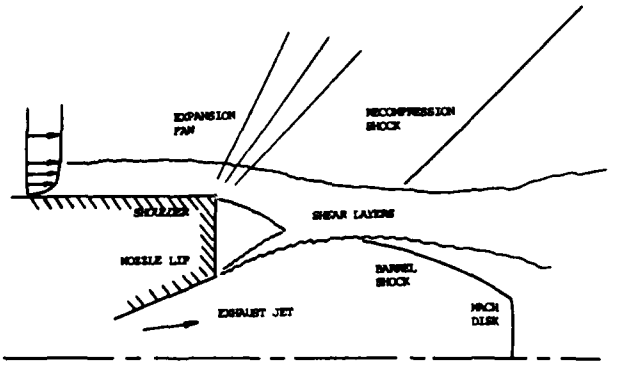

Fig. 1. Sketch of base flow with propulsive jet, showing flow characteristics and nomenclature.

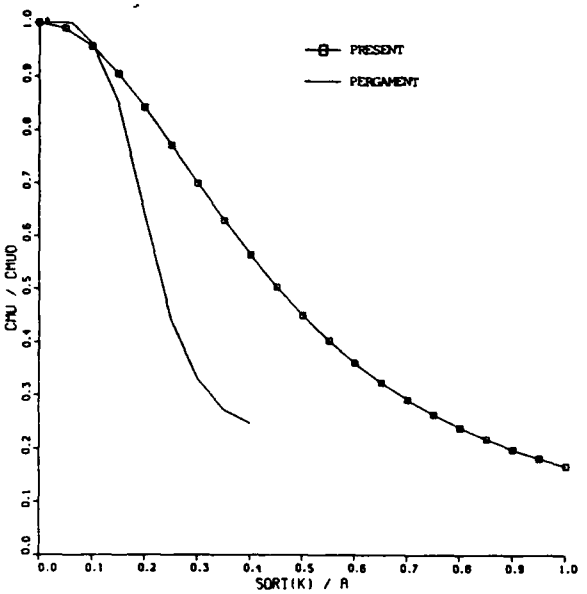

Fig. 2. Modification to k-ε model, $C_\mu/C_{\mu 0}$ as a function of Mach number of velocity fluctuations, present model and from Ref. 15.

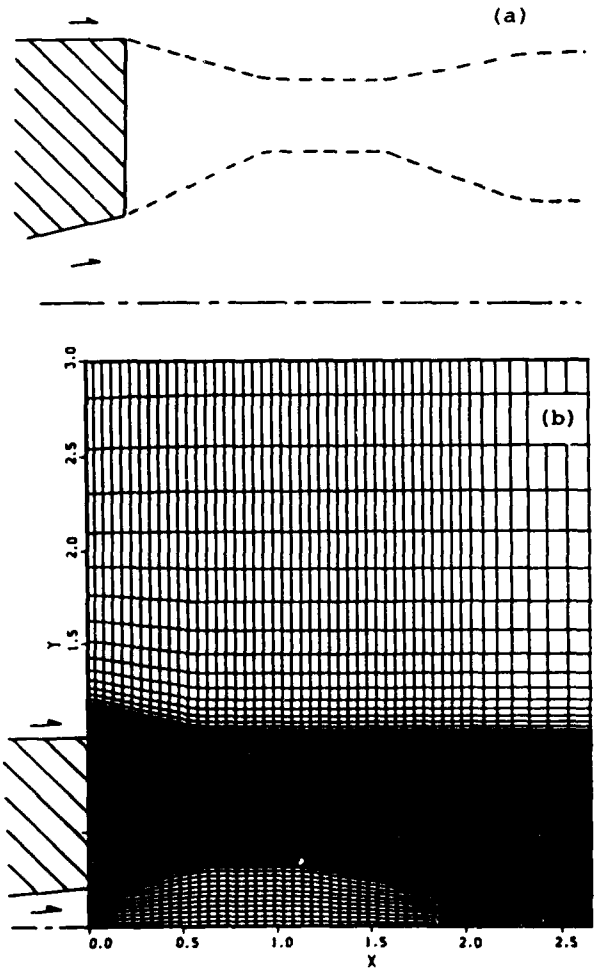

Fig. 3. Typical grid for base flow region produced by clustering at free shear layers adjacent to recirculating flow region, (a) control surfaces, (b) grid.

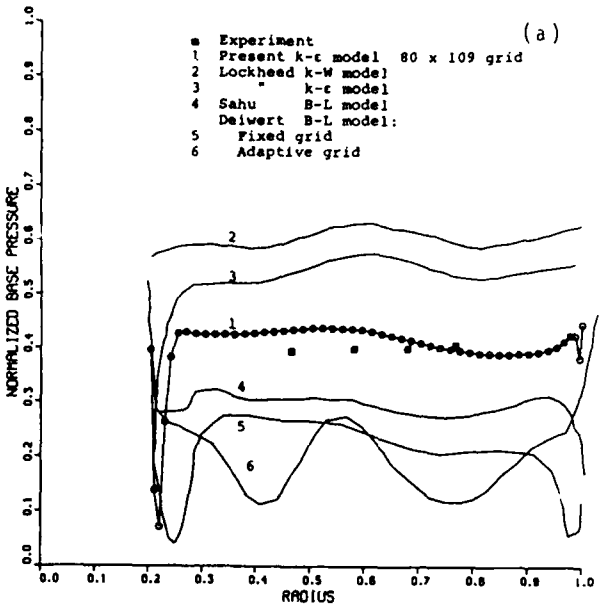

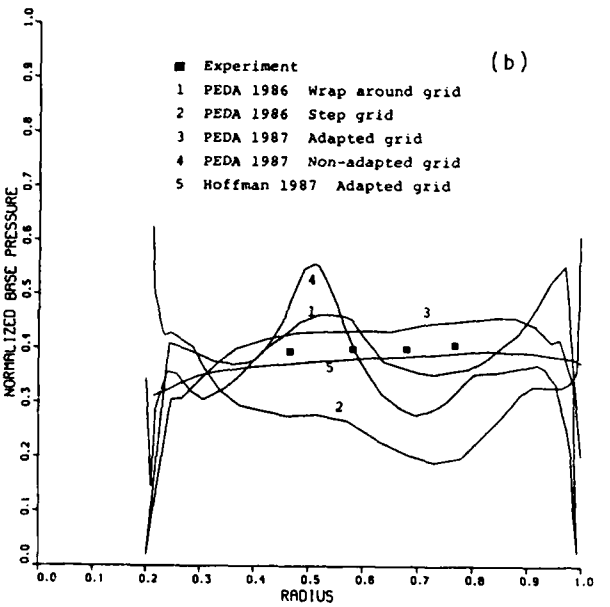

Fig. 4. Comparison of experimental and computational base pressures for (a) present best estimate and "blind" calculations,[1] and (b) other recent results,[7,8,9] NPR = 2.15.

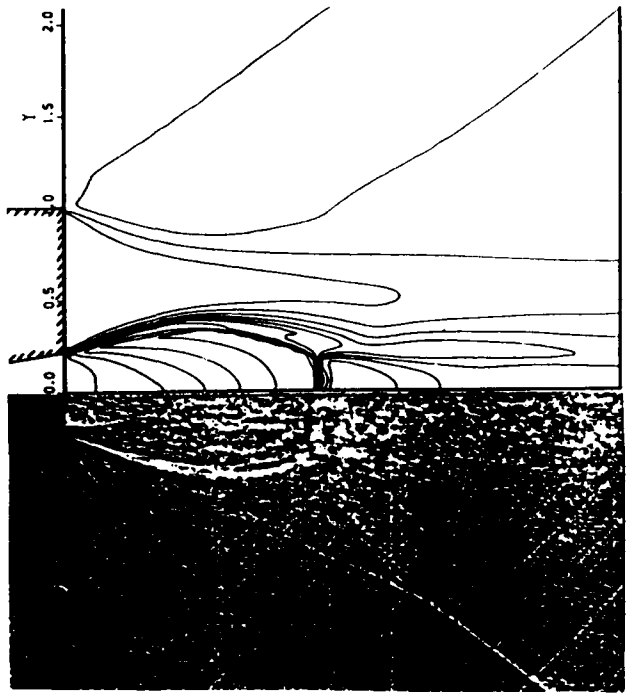

Fig. 5. Comparison of predicted Mach number contours and experimental shadowgraph, NPR = 2.15.

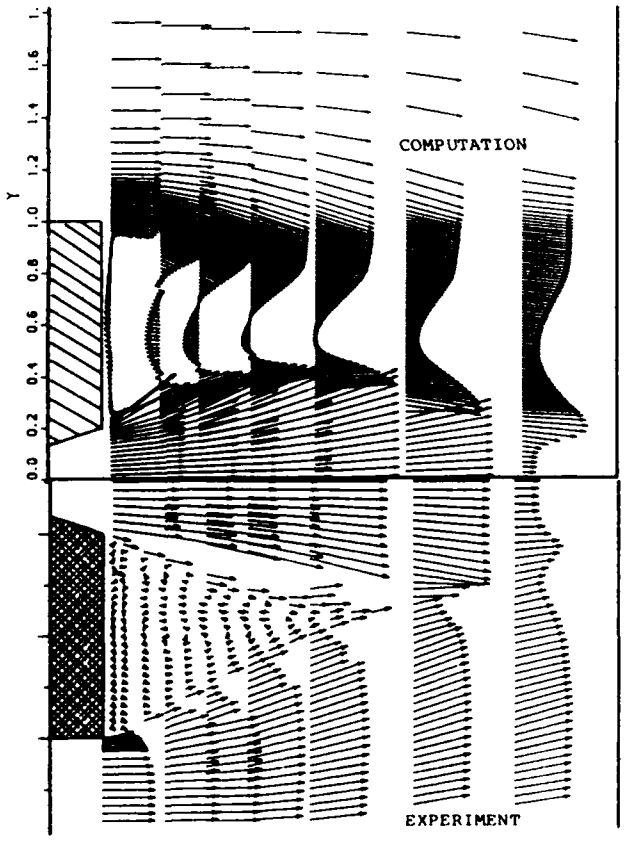

Fig. 6. Comparison of computed and experimental velocity vectors, NPR = 2.15.

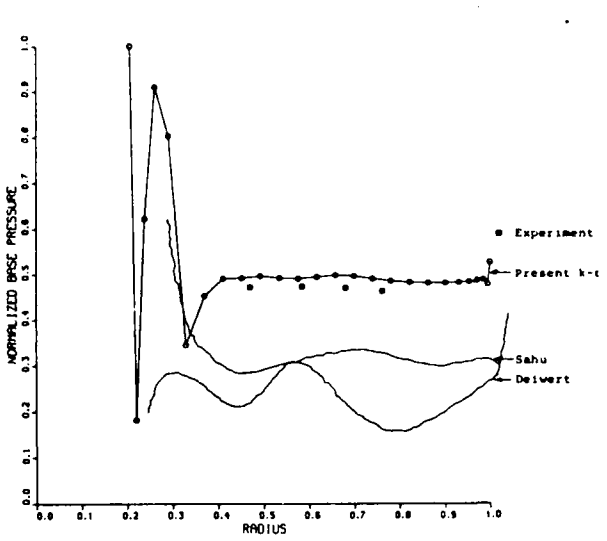

Fig. 7. Comparison of predicted base pressure with experiment and previous calculations,[1] NPR = 6.44.

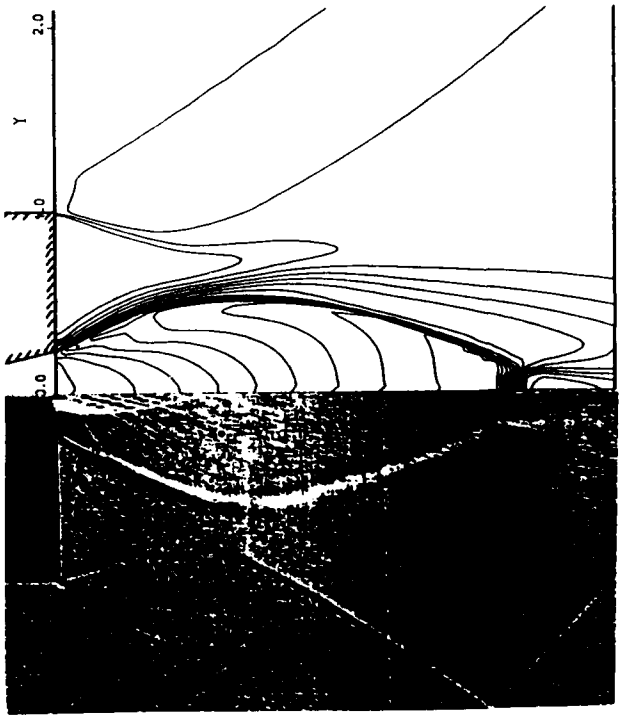

Fig. 8. Comparison of predicted Mach number contours and experimental shadowgraph, NPR = 6.44.

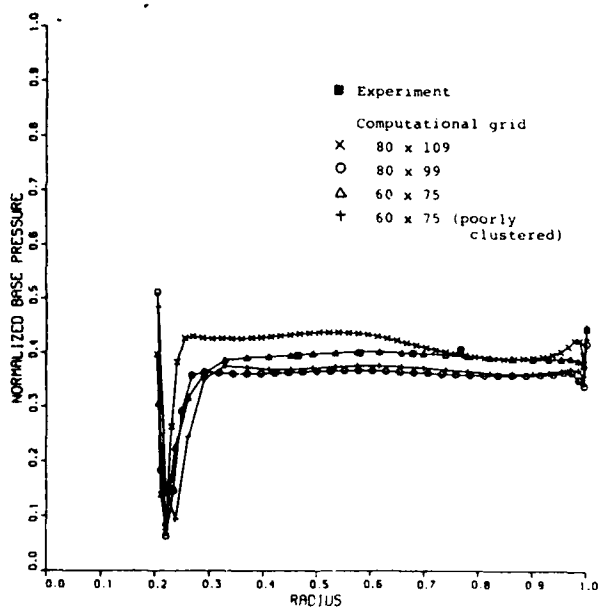

Fig. 9. Range of base pressures predicted by refining grid clustering, for second order upwind differencing scheme, NPR = 2.15

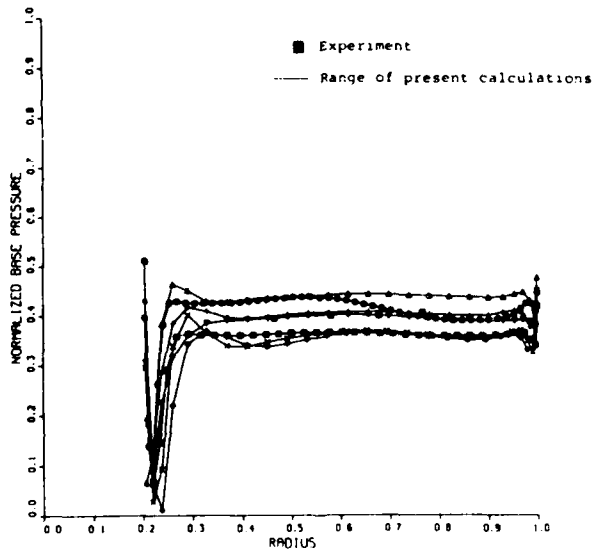

Fig. 10. Range of base pressures predicted by varying grid clustering, differencing scheme, and dissipation parameter used with central differencing, NPR = 2.15

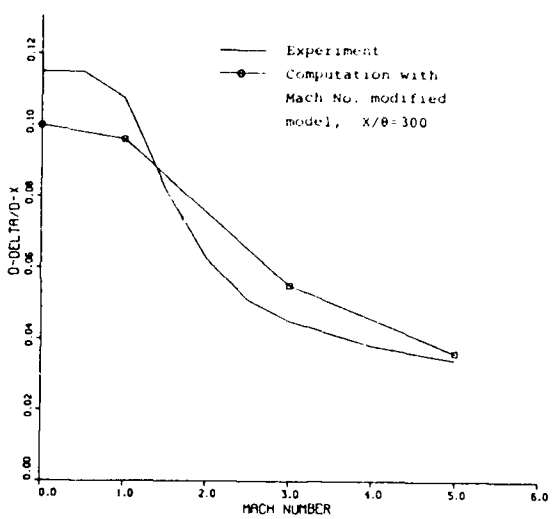

Fig. 11. Spreading rate of a plane free shear layer as a function of Mach number.

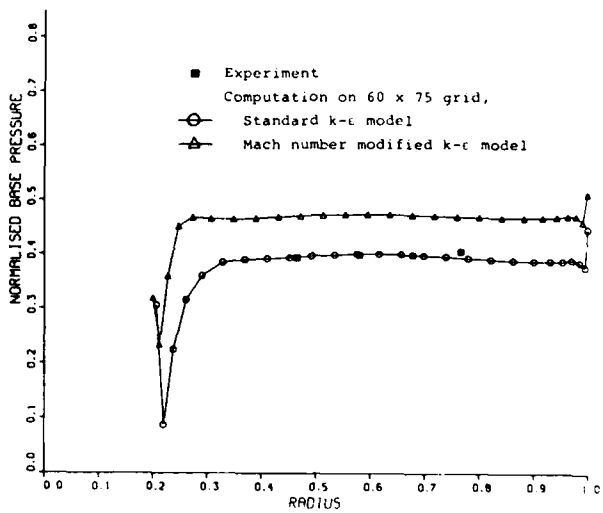

Fig. 12. Effects on computed base pressure of Mach number modification to k-ϵ model, coarse grid calculation, NPR = 2.15.

END

11-87

DTIC